Maximum-Likelihood Source Localization and Unknown Sensor Location Estimation for Wideband Signals in the Near-Field

Joe C. Chen, *Student Member, IEEE*, Ralph E. Hudson, and Kung Yao, *Fellow, IEEE*

***Abstract*—In this paper, we derive the maximum-likelihood (ML) location estimator for wideband sources in the near field of the sensor array. The ML estimator is optimized in a single step, as opposed to other estimators that are optimized separately in relative time-delay and source location estimations. For the multisource case, we propose and demonstrate an efficient alternating projection procedure based on sequential iterative search on single-source parameters. The proposed algorithm is shown to yield superior performance over other suboptimal techniques, including the wideband MUSIC and the two-step least-squares methods, and is efficient with respect to the derived Cramér–Rao bound (CRB). From the CRB analysis, we find that better source location estimates can be obtained for high-frequency signals than low-frequency signals. In addition, large range estimation error results when the source signal is unknown, but such unknown parameter does not have much impact on angle estimation. In some applications, the locations of some sensors may be unknown and must be estimated. The proposed method is extended to estimate the range from a source to an unknown sensor location. After a number of source-location frames, the location of the uncalibrated sensor can be determined based on a least-squares unknown sensor location estimator.**

***Index Terms*—Array shape calibration, beamforming, Cramér–Rao bound, source localization.**

I. Introduction

SOURCE localization using sensor arrays has been one of the central problems in radar, sonar, navigation, geophysics, and acoustic tracking. For the past few decades, a wide variety of techniques have been proposed for the estimation of the direction-of-arrival (DOA) of narrowband sources in the far-field [1]–[5]. In [6], the authors provided an excellent review and comparison of the various narrowband techniques. Recently, there has been an interest in locating wideband sources in the near field, including both the range and the DOA. One obvious application is to locate nearby acoustic sources using a microphone array.

For wideband signals, e.g., acoustic or seismic, the algorithms need to be tailored to account for the large bandwidth. Many have proposed to use focusing matrices to transform the wideband signal subspaces into a predefined narrowband subspace [7]–[9]. Then, the MUSIC algorithm can be applied afterwards as if it was the narrowband case. This class of methods is referred to as the coherent signal subspace method (CSM). Other techniques that evolved from the CSM method include the use of steered covariance matrix [10] and interpolated array [11]. However, the drawback of these methods is the preprocessing that must be performed beforehand. For instance, the CSM methods need to construct the focusing matrices that require focusing angles that are not far from the true DOAs. The interpolated array technique requires the construction of the interpolation matrix, which is also a function of angle. Furthermore, these techniques have never been tested for the near-field case. Recently, an extension of the above methods, but without any preprocessing step, has been studied for the near-field case [12]. It is a natural wideband extension of the conventional MUSIC algorithm; thus, we refer to this method as the wideband MUSIC algorithm and compare it with the proposed method of this paper. It is shown that wideband MUSIC yields poor estimation results (especially in range) for a finite number of data samples (limited due to moving source) and low SNR.

Another class of wideband source localization algorithms is based on time delays (usually for a single source only). These techniques include two independent steps, namely, estimating relative time delays between sensor data and then source location based on the relative time-delay estimates. Closed-form solutions can be derived for the second step based on spherical interpolation [13], [14], hyperbolic intersection [15], or linear intersection [16]. However, these algorithms require the knowledge of the speed of propagation (e.g., the acoustic case). In [17] and [18], closed-form least-squares (LS) and constrained least-squares (CLS) solutions are derived for the case of unknown speed of propagation (e.g., the seismic case). The CLS method improves the performance from that of the LS method by forcing an equality constraint on two components of the unknowns. When the speed of propagation is known, the LS method in [17] and [18], after removing such unknowns, becomes the method independently derived later in [19]. In [19], the authors show that their method is mathematically equivalent to the spherical interpolation technique [13], [14] but with less computational complexity. We refer to the method in [19] as the LS method of known speed of propagation and use it to compare with the proposed method of this paper. In theory, these two-step methods can work for multiple sources, as long as the relative time delays can be estimated from the data. However,

Manuscript received June 11, 2001; revised April 18, 2002. This work was supported in part by the Defense Advanced Research Projects Agency SensIT Program under Contract N66001-00-1-8937, NASA-Dryden under Grant NCC2-374, an UC DIMI grant sponsored by STMicroelectronics, Inc., and a Raytheon Doctoral Fellowship. The associate editor coordinating the review of this paper and approving it for publication was Dr. Joseph Tabrikian.

The authors are with the Electrical Engineering Department, University of California, Los Angeles, CA 90045 USA (e-mail: jcchen@ee.ucla.edu; yao@ee.ucla.edu; ralph@ucla.edu).

Publisher Item Identifier 10.1109/TSP.2002.800420.

this remains to be a challenging task in practice. Recently, the use of higher order statistics to estimate the relative time delays for multiple independent sources has been studied in [20].

In this paper, we derive the "optimal" parametric ML solution to locate wideband sources in the near field. The wideband data is transformed to the frequency domain, and the signal spectrum can be represented by the narrowband model for each frequency bin. This allows a direct optimization for the source location under the assumption of i.i.d. noise instead of the two-step optimization that involves relative time-delay estimation. However, in practice, we apply the DFT, and thus, there are a few artifacts. The circular shift property of the DFT introduces an edge effect problem for the actual linear time shift, and this edge effect is not negligible for a small block of data. To remove the edge effect, appropriate zero padding can be applied. However, it is also known that zero padding destroys the orthogonality of the DFT transform, which makes the noise spectrum appear correlated across frequency. As a result, an exact ML solution for data of finite length does not exist. Instead, we ignore these finite effects and derive the solution, which we refer to as the approximated ML (AML) solution. Note a similar solution has been derived independently in [21] for the far-field case, but here, we consider the near-field case.

In practice, the number of sources must be determined independent of any localization algorithm, but here, we assume it is known for the purpose of this paper. For the single-source case, we show the AML formulation is equivalent to maximizing the sum of the weighted cross-correlation functions between time shifted sensor data. The optimization using all sensor pairs mitigates the ambiguity problem that often arises in the relative time-delay estimation between two widely separated sensors for the two-step LS methods. In the case of multiple sources, we apply an efficient alternating projection (AP) procedure, which avoids the multidimensional search by sequentially estimating the location of one source while fixing the estimates of other source locations from the previous iteration.

Besides the development of the AML method, we also derive the theoretical Cramér–Rao bound (CRB) for both performance comparison and basic understanding purposes. The CRB shows that the localization variance bound can be broken down into two separate parts: one that depends on the signal characteristics and one that depends on the array geometry. The signal dependent part shows that theoretically, the source location RMS error is linearly proportional to the noise level and the speed of propagation and inversely proportional to the source spectrum and frequency. Thus, better source location estimates can be obtained for high-frequency signals than low-frequency signals. In further sensitivity analysis, large range estimation error is found when the source signal is unknown, but such an unknown parameter does not affect the angle estimation.

It is well known that the performance of source localization degrades when the sensor locations are in error. This problem arises in many cases where the sensors may be randomly deployed in an ad hoc network or even move to different positions in time. The estimation of unknown sensor locations, which are often called array shape calibration, has also drawn considerable attention in the literature [22]–[25]. In the later section of this paper, we extend the AML source localization algorithm to output an estimate of the range from a source to one or more sensors of unknown locations. When several ranges from different source locations are accumulated, they can be combined by a least-squares calibration (LSC) method to estimate the unknown sensor locations. This extended AML method shows promising improvement over our previous method based on LS source localization [26]. Other issues such as calibrating the sensor gain, phase, mutual coupling, and channel mismatch are also critical in practice, but we ignore them for the purpose of this paper.

The paper is organized as follows. In Section II, we derive the AML solution for source localization. Then, the CRB for source localization is derived in Section III. In Section IV, the LSC unknown sensor location estimation is introduced. Then, simulation examples and systematic evaluations are provided to show the effectiveness of the proposed algorithms in Section V. Finally, we give our conclusions.

II. Maximum-Likelihood Source Localization

A. Derivation of the AML Solution

The derivation of the AML solution for real-valued signals generated by wideband sources in the near field is an extension of the classical maximum-likelihood DOA estimator for narrowband signals. Due to the wideband nature of the signal, the AML metric results in a combination of each subband. Since we consider near-field sources, the signal strength at each sensor can be different due to nonuniform spatial loss in the near-field geometry. The sensors are assumed to be omnidirectional and have identical responses. For a randomly distributed array of R sensors, the data collected by the pth sensor at time n can be given by

$$x_p(n) = \sum_{m=1}^{M} a_p^{(m)} s_0^{(m)} \left(n - t_p^{(m)}\right) + w_p(n) \qquad (1)$$

for $n = 0, \ldots, L-1$, $p = 1, \ldots, R$, and $m = 1, \ldots, M$, where

- M number of sources (assumed to be known and $M < R$);
- $a_p^{(m)}$ signal gain level of the mth source at the pth sensor (assumed to be constant within the block of data);
- $s_0^{(m)}$ source signal;
- $t_p^{(m)}$ fractional time-delay in samples (which is allowed to be any real-valued number);
- w_p zero mean i.i.d. Gaussian noise with variance σ^2.

The time delay is defined by $t_p^{(m)} = \|\mathbf{r}_{s_m} - \mathbf{r}_p\|/v$, where

- $\mathbf{r}_{s_m}$ mth source location;
- $\mathbf{r}_p$ pth sensor location;
- v speed of propagation in length unit per sample.

Define the relative time-delay between the pth and the qth sensors by $t_{pq}^{(m)} = t_p^{(m)} - t_q^{(m)} = (\|\mathbf{r}_{s_m} - \mathbf{r}_p\| - \|\mathbf{r}_{s_m} - \mathbf{r}_q\|)/v$. A block of L samples in each sensor data can be transformed to the frequency domain by a DFT of length N. As discussed earlier, the DFT creates a circular time shift rather than the actual time shift. When $N = L$, severe edge effect results for small L, but it becomes a good approximation for large L. We can apply zero padding for small L to remove such edge effect, i.e., $N \geq L + \tau$, where τ is the maximum relative time-delay among

all sensor pairs. However, the zero-padding removes the orthogonality of the noise component across frequency. In practice, the size of L is limited due to the nonstationarity of the source location. Thus, in the following derivation, we assume that either L is large enough or that the noise is almost uncorrelated across frequency and claim such a formulation as an approximation to the maximum-likelihood solution. Throughout this paper, we denote superscript T as the transpose, H as the complex conjugate transpose, and $*$ as the complex conjugate operation.

In the frequency domain, the array signal model is given by

$$\mathbf{X}(k) = \mathbf{D}(k)\mathbf{S}_0(k) + \eta(k) \tag{2}$$

for $k = 0, \ldots, N-1$, where the array data spectrum is given by $\mathbf{X}(k) = [X_1(k), \ldots, X_R(k)]^T$, the steering matrix is given by $\mathbf{D}(k) = [\mathbf{d}^{(1)}(k), \ldots, \mathbf{d}^{(M)}(k)]$, the steering vector is given by $\mathbf{d}^{(m)}(k) = [d_1^{(m)}(k), \ldots, d_R^{(m)}(k)]^T$, $d_p^{(m)}(k) = a_p^{(m)} e^{-j2\pi k t_p^{(m)}/N}$, and the source spectrum is given by $\mathbf{S}_0(k) = [S_0^{(1)}(k), \ldots, S_0^{(M)}(k)]^T$. The noise spectrum vector $\eta(k)$ is zero mean complex white Gaussian distributed with variance $L\sigma^2$ in each element. Note due to the transformation to the frequency domain, $\eta(k)$ asymptotically approaches a Gaussian distribution by the central limit theorem, even if the actual time-domain noise has an arbitrary i.i.d. distribution (with bounded variance) other than Gaussian. This asymptotic property in the frequency domain provides a more reliable noise model than the time-domain model in some practical cases. For convenience of notation, we define $\mathbf{S}(k) = \mathbf{D}(k)\mathbf{S}_0(k)$. By stacking up the $N/2$ positive frequency bins (zero frequency bin is not important and the negative frequency bins are merely mirror images) of the signal model in (2) into a single column, we can rewrite the sensor data into a $NR/2 \times 1$ space–temporal frequency vector as $\mathbf{X} = \mathbf{G}(\Theta) + \xi$, where $\mathbf{G}(\Theta) = [\mathbf{S}(1)^T, \ldots, \mathbf{S}(N/2)^T]^T$, and $\mathbf{R}_\xi = E[\xi\xi^H] = L\sigma^2\mathbf{I}_{NR/2}$. We assume, initially, that the unknown parameter space is $\Theta = [\tilde{\mathbf{r}}_s{}^T, \mathbf{S}_0^{(1)^T}, \ldots, \mathbf{S}_0^{(M)^T}]^T$, where the source locations are denoted by $\tilde{\mathbf{r}}_s = [\mathbf{r}_{s_1}^T, \ldots, \mathbf{r}_{s_M}^T]^T$, and the source signal spectrum is denoted by $\mathbf{S}_0^{(m)} = [S_0^{(m)}(1), \ldots, S_0^{(m)}(N/2)]^T$. The signal gain levels $a_p^{(m)}$ are assumed to be known in this derivation, and the effect of not knowing $a_p^{(m)}$ will be discussed in a later section. The log-likelihood function of the complex Gaussian noise vector ξ, after ignoring irrelevant constant terms, is given by $\mathcal{L}(\Theta) = -||\mathbf{X} - \mathbf{G}(\Theta)||^2$. The maximum-likelihood estimation of the source locations and source signals is given by the following optimization criterion:

$$\max_{\Theta} \mathcal{L}(\Theta) = \min_{\Theta} \sum_{k=1}^{N/2} ||\mathbf{X}(k) - \mathbf{D}(k)\mathbf{S}_0(k)||^2 \tag{3}$$

which is equivalent to finding $\min_{\tilde{\mathbf{r}}_s, \mathbf{S}_0(k)} f(k)$ for all k bins, where

$$f(k) = ||\mathbf{X}(k) - \mathbf{D}(k)\mathbf{S}_0(k)||^2. \tag{4}$$

The minima of $f(k)$ with respect to the source signal vector $\mathbf{S}_0(k)$ must satisfy $\partial f(k)/\partial \mathbf{S}_0^H(k) = 0$; hence, the estimate of the source signal vector that yields the minimum residual at any source location is given by

$$\hat{\mathbf{S}}_0(k) = \mathbf{D}^\dagger(k)\mathbf{X}(k) \tag{5}$$

where $\mathbf{D}^\dagger(k) = (\mathbf{D}(k)^H\mathbf{D}(k))^{-1}\mathbf{D}(k)^H$ is the pseudo-inverse of the steering matrix $\mathbf{D}(k)$. Define the orthogonal projection $\mathbf{P}(k, \tilde{\mathbf{r}}_s) = \mathbf{D}(k)\mathbf{D}^\dagger(k)$ and the complement orthogonal projection $\mathbf{P}^\perp(k, \tilde{\mathbf{r}}_s) = \mathbf{I} - \mathbf{P}(k, \tilde{\mathbf{r}}_s)$. By substituting (5) into (4), the minimization function becomes $f(k) = ||\mathbf{P}^\perp(k, \tilde{\mathbf{r}}_s)\mathbf{X}(k)||^2$. After substituting the estimate of $\mathbf{S}_0(k)$, the AML source locations estimate can be obtained by solving the following maximization problem:

$$\max_{\tilde{\mathbf{r}}_s} J(\tilde{\mathbf{r}}_s) = \max_{\tilde{\mathbf{r}}_s} \sum_{k=1}^{N/2} ||\mathbf{P}(k, \tilde{\mathbf{r}}_s)\mathbf{X}(k)||^2. \tag{6}$$

Note that the AML metric $J(\tilde{\mathbf{r}}_s)$ has an implicit form for the estimation of $\mathbf{S}_0(k)$, whereas the metric $\mathcal{L}(\Theta)$ shows the explicit form. Once the AML estimate of $\tilde{\mathbf{r}}_s$ is obtained, the AML estimate of the source signals can be given by (5). It is interesting that when zero-padding is applied, the covariance matrix $\mathbf{R}_\xi$ is no longer diagonal and is indeed singular; thus, an exact ML solution cannot be derived without the inverse of $\mathbf{R}_\xi$. In the above formulation, we derive the AML solution using only a single block. A different AML solution using multiple blocks could also be formed with some possible computational advantages. When the speed of propagation is unknown, as in the case of seismic media, we may expand the unknown parameter space to include it, i.e., $\Theta = [\tilde{\mathbf{r}}_s{}^T, v]^T$.

B. Single-Source Case

In the single-source case, the AML metric in (6) becomes $J(\mathbf{r}_s) = \sum_{k=1}^{N/2} |B(k, \mathbf{r}_s)|^2$, where $B(k, \mathbf{r}_s) = \overline{\mathbf{d}}(k, \mathbf{r}_s)^H\mathbf{X}(k)$ is the beam-steered beamformer output in the frequency-domain [27], $\overline{\mathbf{d}} = \mathbf{d}/\sqrt{\sum_{p=1}^R a_p^2}$ is the normalized steering vector, and $\overline{a}_p = a_p/\sqrt{\sum_{p=1}^R a_p^2}$ is the normalized signal gain level at the pth sensor. It is interesting to note that in the near-field case, the AML beamformer output is the result of forming a focused spot (or area) on the source location rather than a beam since range is also considered. In Appendix A, the AML criterion is shown to be equivalent to maximizing the weighted cross correlations between sensor data, which is commonly used for estimating relative time delays.

The source location can be estimated based on where $J(\mathbf{r}_s)$ is maximized for a given set of locations. Define the normalized metric

$$J_N(\mathbf{r}_s) \equiv \frac{\sum_{k=1}^{N/2} |B(k, \mathbf{r}_s)|^2}{J_{\max}} \leq 1 \tag{7}$$

where $J_{\max} = \sum_{k=1}^{N/2} [\sum_{p=1}^R \overline{a}_p |X_p(k)|]^2$, which is useful to verify estimated peak values. Without any prior information on possible region of the source location, the AML metric should be evaluated on a set of grid points. A nonuniform grid is suggested to reduce the number of grid points. For the 2-D case,

polar coordinates with nonuniform sampling of the range and uniform sampling of the angle can be transformed to Cartesian coordinates that are dense near the array and sparse away from the array. When the crude estimate of the source location is obtained from the grid-point search, iterative methods can be applied to reach the global maximum (without running into local maxima given appropriate choice of grid points). In some cases, grid-point search is not necessary since a good initial location estimate is available, e.g., from the estimate of the previous data frame for a slowly moving source. One simple iterative gradient algorithm can be formulated in the following:

$$\mathbf{r}_s^{(i+1)} = \mathbf{r}_s^{(i)} + \mu \left[\nabla_{\mathbf{r}_s} J_{\mathrm{N}} \left(\mathbf{r}_s^{(i)} \right) \right] \tag{8}$$

where μ is the step size that depends on the shape of $J_{\mathrm{N}}(\mathbf{r}_s)$ and initial estimate $\mathbf{r}_s^{(0)}$

$$\nabla_{\mathbf{r}_s} J_{\mathrm{N}}(\mathbf{r}_s) = \frac{-4\pi}{J_{\max} N v} \sum_{k=1}^{N/2} k \mathrm{Im} \left[B^*(k, \mathbf{r}_s) \mathbf{C}(k, \mathbf{r}_s) \right] \tag{9}$$

is the gradient of the normalized $J_{\mathrm{N}}(\mathbf{r}_s)$, $\mathbf{C}(k, \mathbf{r}_s) = \sum_{p=1}^{R} \overline{a}_p X_p(k) c^{j2\pi k t_p / N} \mathbf{u}_p$, and $\mathbf{u}_p = (\mathbf{r}_s - \mathbf{r}_p)/\|\mathbf{r}_s - \mathbf{r}_p\|$. Other advanced and robust methods may be used without specifying a step size, e.g., the Nelder–Mead direct search method [28]. Note that the efficiency and complexity of these iterative methods are beyond the scope of this paper and, thus, will not be discussed.

Note that in the derivation of the AML solution, we have assumed known sensor gain levels a_p, or the normalized sensor gains $\overline{a}_p$, for $p = 1, \ldots, R$. However, in practice, they are also unknown. The signal model in the far-field case usually ignores this scale factor since the SNR is assumed to be uniform across the array when the source is far away (for omni-directional sensors). When the source is in the near field, the SNR at each sensor is different due to the different spatial loss from the source to each sensor. Thus, the maximization on the AML metric $J(\mathbf{r}_s)$ is indeed based on a weighted least-squares criterion, where each sensor data is weighted by its signal strength in the overall metric. When the $\overline{a}_p$ are unknown, they can be replaced by their estimates. Two simple but biased estimators using the ℓ_1 and ℓ_2 norms for the $\overline{a}_p$ can be given by $\hat{\overline{a}}_p{}^{(\ell_1)} = \sum_{n=0}^{L-1} |x_p(n)| / \sum_{p=1}^{R} \sum_{n=0}^{L-1} |x_p(n)|$ and $\hat{\overline{a}}_p{}^{(\ell_2)} = \sum_{n=0}^{L-1} x_p^2(n) / \sum_{p=1}^{R} \sum_{n=0}^{L-1} x_p^2(n)$, respectively. In Appendix B, an extended AML solution is derived to incorporate unknown $\overline{a}_p$ for the single-source case. It is shown that the extended AML metric involves finding the principle singular value of a newly defined data spectrum matrix. The resulting source location estimate using this metric yields a weighted least-squares solution, where the $\overline{a}_p$ are also implicitly estimated at the same time. Although this new metric can effectively estimate the sensor gain levels, we find that the source location estimation degrades when we expand the parameter space to include the $\overline{a}_p$. Based on our simulation results, we find that it is better to use separately estimated $\overline{a}_p$ or simply assume uniform gains, i.e., $\overline{a}_p = 1$, for the single source AML method. The uniform gain assumption makes the AML solution a least-squares one instead of a weighted least-squares one. However, we find that such an assumption does not give much performance degradation for the single-source case when the actual gain is merely modeled by the spatial loss.

C. Multiple-Source Case

For the multiple-source case, the parameter estimation is a challenging task. Although iterative multidimensional parameter search methods, such as the Nelder–Mead direct search method, can be applied to avoid an exhaustive multidimensional grid search, finding the initial source location estimates is not trivial. Since iterative solutions for the single-source case are more robust and the initial estimate is easier to find, we extend the alternating projection method in [2] to the near-field problem. The alternating projection approach breaks the multidimensional parameter search into a sequence of single source parameter search and yields fast convergence rate. The following describes the alternating projection algorithm for the two-source case, but it can be easily extended to the case of M sources.

Alternating Projection Algorithm:

Step 1) Estimate the location of the stronger source on a single source grid

$$\mathbf{r}_{s_1}^{(0)} = \arg \max_{\mathbf{r}_{s_1}} J(\mathbf{r}_{s_1}). \tag{10}$$

Step 2) Estimate the location of the weaker source on a single source grid under the assumption of a two-source model while keeping the first source location estimate from step 1) constant:

$$\mathbf{r}_{s_2}^{(0)} = \arg \max_{\mathbf{r}_{s_2}} J\left(\left[\mathbf{r}_{s_1}^{(0)^T}, \mathbf{r}_{s_2}^T \right]^T \right). \tag{11}$$

For $i = 1, \ldots$, repeat steps 3) and 4) until convergence.

Step 3) Do an iterative AML parameter search (direct search or gradient) for the location of the first source while keeping the estimate of the second source location from the previous iteration constant:

$$\mathbf{r}_{s_1}^{(i)} = \arg \max_{\mathbf{r}_{s_1}} J\left(\left[\mathbf{r}_{s_1}^T, \mathbf{r}_{s_2}^{(i-1)^T} \right]^T \right). \tag{12}$$

Step 4) Do an iterative AML parameter search (direct search or gradient) for the location of the second source while keeping the estimate of the first source location from step 3) constant:

$$\mathbf{r}_{s_2}^{(i)} = \arg \max_{\mathbf{r}_{s_2}} J\left(\left[\mathbf{r}_{s_1}^{(i)^T}, \mathbf{r}_{s_2}^T \right]^T \right). \tag{13}$$

Similar to the single-source case, the sensor gain levels $a_p^{(m)}$ can be nonuniform and unknown when all the sources are in the near field. However, when there are multiple sources, the gains are not easily determined (still an open issue). Thus, we may assume uniform gains, i.e., $a_p^{(m)} = 1$. In our simulations, when the signal gains are modeled by the spatial loss, we find the location estimates of two sources to be off from the actual locations by quite a significant amount. Therefore, the gains $a_p^{(m)}$ are crucial parameters in the multisource case, as opposed to the single-source case.

III. Cramér–Rao Bound for Source Localization

The CRB is most often used as a theoretical lower bound for any unbiased estimator [29]. Most of the derivations of the CRB for wideband source localization found in the literature are in terms of relative time-delay estimation error. In this section, we derive a more general CRB directly from the signal model. By developing a theoretical lower bound in terms of signal characteristics and array geometry, we not only bypass the involvement of the intermediate time-delay estimator but also offer useful insights into the physics of the problem.

We consider the following three cases:

1) known signal and known speed of propagation;
2) known signal but unknown speed of propagation;
3) known speed of propagation but unknown signal.

The comparison of the three conditions (see Section V) provides a sensitivity analysis that explains the fundamental differences of different problems, e.g., unknown speed of propagation for seismic sensing and known signal for some applications. The case of unknown signal and unknown speed of propagation is not too different from the case of unknown signal and known speed of propagation; thus, it is not considered. For all cases, we can construct the Fisher information matrix [29] from the signal model defined in Section II by

$$\mathbf{F} = 2\mathrm{Re}\left[\mathbf{H}^H\mathbf{R}_\xi^{-1}\mathbf{H}\right] = \left(2/L\sigma^2\right)\mathrm{Re}\left[\mathbf{H}^H\mathbf{H}\right] \tag{14}$$

where $\mathbf{H} = \partial\mathbf{G}/\partial\mathbf{r}_s^T$ for the first case, assuming that $\mathbf{r}_s$ is the only unknown in the single-source case. In this case, $\mathbf{F}_{\mathbf{r}_s} = \zeta\mathbf{A}$, where $\zeta = (2/L\sigma^2v^2)\sum_{k=1}^{N/2}(2\pi k|S_0(k)|/N)^2$ is the scale factor that is proportional to the total power in the derivative of the source signal

$$\mathbf{A} = \sum_{p=1}^{R} a_p^2\mathbf{u}_p\mathbf{u}_p^T \tag{15}$$

is the *array matrix,* and $\mathbf{u}_p = (\mathbf{r}_s - \mathbf{r}_p)/\|\mathbf{r}_s - \mathbf{r}_p\|$ is the unit vector indicating the direction of the source from the pth sensor. The $\mathbf{A}$ matrix provides a measure of geometric relations between the source and the sensor array. Poor array geometry may lead to degeneration in the rank of matrix $\mathbf{A}$. It is clear from the scale factor ζ, as will be shown later, that the performance does not solely depend on the SNR but also the signal bandwidth and spectral density. Thus, source localization performance is better for signals with more energy in the high frequencies.

For the second case, when the speed of propagation is also unknown, i.e., $\Theta = [\mathbf{r}_s^T, v]^T$, the $\mathbf{H}$ matrix for this case is given by $\mathbf{H} = [\partial\mathbf{G}/\partial\mathbf{r}_s^T, \partial\mathbf{G}/\partial v]$. The Fisher information block matrix is given by

$$\mathbf{F}_{\mathbf{r}_s, v} = \zeta\begin{bmatrix}\mathbf{A} & -\mathbf{U}\mathbf{A}_a\mathbf{t}\\ -\mathbf{t}^T\mathbf{A}_a\mathbf{U}^T & \mathbf{t}^T\mathbf{A}_a\mathbf{t}\end{bmatrix} \tag{16}$$

where $\mathbf{U} = [\mathbf{u}_1, \ldots, \mathbf{u}_R]$, $\mathbf{A}_a = \mathrm{diag}([a_1^2, \ldots, a_R^2])$, and $\mathbf{t} = [t_1, \ldots, t_R]^T$. By applying the well-known block matrix inversion lemma (see [30, App.]), the leading $D \times D$ submatrix of the inverse Fisher information block matrix can be given by

$$\left[\mathbf{F}_{\mathbf{r}_s, v}^{-1}\right]_{11:DD} = \frac{1}{\zeta}\left(\mathbf{A} - \mathbf{Z}_v\right)^{-1} \tag{17}$$

where the *penalty matrix* due to unknown speed of propagation is defined by $\mathbf{Z}_v = (1/\mathbf{t}^T\mathbf{A}_a\mathbf{t})\mathbf{U}\mathbf{A}_a\mathbf{t}\mathbf{t}^T\mathbf{A}_a\mathbf{U}^T$. The matrix $\mathbf{Z}_v$ is non-negative definite; therefore, the source localization error of the unknown speed of propagation case is always larger than that of the known case.

For the third case, when the source signal is also unknown, i.e., $\Theta = [\mathbf{r}_s^T, |\mathbf{S}_0|^T, \mathbf{\Phi}_0^T]^T$, the $\mathbf{H}$ matrix is given by $\mathbf{H} = [\partial\mathbf{G}/\partial\mathbf{r}_s^T, \partial\mathbf{G}/\partial|\mathbf{S}_0|^T, \partial\mathbf{G}/\partial\mathbf{\Phi}_0^T]$, where $\mathbf{S}_0 = [S_0(1), \ldots, S_0(N/2)]^T$, and $|\mathbf{S}_0|$ and $\mathbf{\Phi}_0$ are the magnitude and phase part of $\mathbf{S}_0$, respectively. The Fisher information matrix can then be explicitly given by

$$\mathbf{F}_{\mathbf{r}_s, \mathbf{S}_0} = \begin{bmatrix}\zeta\mathbf{A} & \mathbf{B}\\ \mathbf{B}^T & \mathbf{D}\end{bmatrix} \tag{18}$$

where $\mathbf{B}$ and $\mathbf{D}$ are not explicitly given since they are not needed in the final expression. By applying the block matrix inversion lemma, the leading $D \times D$ submatrix of the inverse Fisher information block matrix can be given by

$$\left[\mathbf{F}_{\mathbf{r}_s, \mathbf{S}_0}^{-1}\right]_{11:DD} = \frac{1}{\zeta}\left(\mathbf{A} - \mathbf{Z}_{\mathbf{S}_0}\right)^{-1} \tag{19}$$

where the penalty matrix due to unknown source signal is defined by

$$\mathbf{Z}_{\mathbf{S}_0} = \frac{1}{\sum_{p=1}^{R} a_p^2}\left(\sum_{p=1}^{R} a_p^2\mathbf{u}_p\right)\left(\sum_{p=1}^{R} a_p^2\mathbf{u}_p\right)^T. \tag{20}$$

The CRB with unknown source signal is always larger than that with known source signal, as discussed later. This can be easily shown since the penalty matrix $\mathbf{Z}_{\mathbf{S}_0}$ is non-negative definite. The $\mathbf{Z}_{\mathbf{S}_0}$ matrix acts as a penalty term since it is the average of the square of weighted $\mathbf{u}_p$ vectors. The estimation variance is larger when the source is far away since the $\mathbf{u}_p$ vectors are similar in directions to generate a larger penalty matrix, i.e., $\mathbf{u}_p$ vectors add up. When the source is inside the convex hull of the sensor array, the estimation variance is smaller since $\mathbf{Z}_{\mathbf{S}_0}$ approaches the zero matrix, i.e., $\mathbf{u}_p$ vectors cancel each other. For the 2-D case, the CRB for the distance error of the estimated location $[\hat{x}_s, \hat{y}_s]^T$ from the true source location can be given by

$$\sigma_d^2 = \sigma_{x_s}^2 + \sigma_{y_s}^2 \geq \left[\mathbf{F}_{\mathbf{r}_s, \mathbf{S}_0}^{-1}\right]_{11} + \left[\mathbf{F}_{\mathbf{r}_s, \mathbf{S}_0}^{-1}\right]_{22} \tag{21}$$

where $d^2 = (\hat{x}_s - x_s)^2 + (\hat{y}_s - y_s)^2$. By further expanding the parameter space, the CRB for multiple source localizations can also be derived, but its analytical expression is much more complicated. Note that when both the source signal and sensor gains are unknown, it is not possible to determine the values of the source signal and the sensor gains (they can only be estimated up to a scaled constant).

By transforming to the polar coordinate system in the 2-D case, the CRB for the source range and DOA can also be given. Denote $r_s = \sqrt{x_s^2 + y_s^2}$ as the source range from a reference position such as the array centroid. The DOA can be given by $\phi_s = \tan^{-1}(x_s/y_s)$ with respect to the Y-axis. The time delay from the source to the pth sensor is then given by $t_p = \sqrt{r_s^2 + r_p^2 - 2r_sr_p\cos(\phi_s - \phi_p)}/v$, where (r_p, ϕ_p) is

the polar position of the pth sensor. We can form a polar array matrix $\mathbf{A}^{\text{pol}} = \sum_{p=1}^{R} a_p^2 \mathbf{v}_p \mathbf{v}_p^T$, where

$$\mathbf{v}_p = \left[\frac{r_s - r_p \cos(\phi_s - \phi_p)}{\|\mathbf{r}_s - \mathbf{r}_p\|}, \frac{r_s r_p \sin(\phi_s - \phi_p)}{\|\mathbf{r}_s - \mathbf{r}_p\|} \right]^T. \quad (22)$$

Similarly, the polar penalty matrix due to unknown source signal can be given by

$$\mathbf{Z}_{\mathbf{S}_0}^{\text{pol}} = \frac{1}{\sum_{p=1}^{R} a_p^2} \left(\sum_{p=1}^{R} a_p^2 \mathbf{v}_p \right) \left(\sum_{p=1}^{R} a_p^2 \mathbf{v}_p \right)^T. \quad (23)$$

The leading 2×2 submatrix of the inverse polar Fisher information block matrix can be given by

$$\left[\mathbf{F}^{-1}_{(r_s, \phi_s), \mathbf{S}_0} \right]_{11:22} = \frac{1}{\zeta} \left(\mathbf{A}^{\text{pol}} - \mathbf{Z}_{\mathbf{S}_0}^{\text{pol}} \right)^{-1}. \quad (24)$$

Then, the lower bound of range estimation variance can be given by $\sigma_{r_s}^2 \geq [\mathbf{F}^{-1}_{(r_s, \phi_s), \mathbf{S}_0}]_{11}$ and the lower bound of DOA estimation variance can be given by $\sigma_{\phi_s}^2 \geq [\mathbf{F}^{-1}_{(r_s, \phi_s), \mathbf{S}_0}]_{22}$. The polar array matrix shows that a good DOA estimate can be obtained at the broadside of a linear array, and a poor DOA estimate results at the endfire of a linear array. A two-dimensional (2-D) array is required for better range and DOA estimations, e.g., a circular array.

IV. Unknown Sensor Location Estimation

In this section, we propose a method for estimating the unknown sensor location using an extended AML method followed by the LSC method. Although the following formulation is only for a single sensor of unknown location, it can be extended to estimate other unknown sensor locations in sequential steps one at a time. We assume the locations of R sensors are known *a priori*, but the calibrating source is an unknown signal at an unknown location (i.e., online calibration). The AML estimator is extended to include the parameters $\Theta = [\mathbf{r}_s^T, d]^T$, where $d = \|\mathbf{r}_s - \mathbf{r}_u\|$ is the distance from the source to the unknown sensor location $\mathbf{r}_u$. The source location is estimated using the R sensors of known locations, and the distance d is estimated using the sensor of unknown location. Only the distance d is added to the parameter space since an ambiguity exists in a circle around the source. The extended AML metric can be given by $\tilde{J}(\Theta) = \sum_{k=1}^{N/2} |\overline{\mathbf{d}}(k)^H \tilde{\mathbf{X}}(k)|^2$, where $\overline{\mathbf{d}}(k) = [\overline{\mathbf{d}}(k)^T, \overline{a}_u e^{-j2\pi k d/Nv}]^T$, $\tilde{\mathbf{X}}(k) = [\mathbf{X}(k)^T, X_u(k)]^T$, $X_u(k)$ is the data spectrum of the sensor of unknown location, and $\overline{a}_u$ is the normalized sensor gain level at this sensor.

For the 2-D case, the unknown sensor location $\mathbf{r}_u$ can be obtained by the intersection of the circles drawn from three or more source locations, as depicted in Fig. 1. The estimation then becomes a two-step process. The extended AML method is used to sequentially estimate M sets of parameters, i.e., $[\mathbf{r}_{s_1}^T, d_1]^T, \ldots, [\mathbf{r}_{s_M}^T, d_M]^T$, where $M \geq 3$ is the number of sources. Note that the estimation of these parameters can be done either separately or jointly for all sources, but we only consider the separate case for simplicity. The source locations

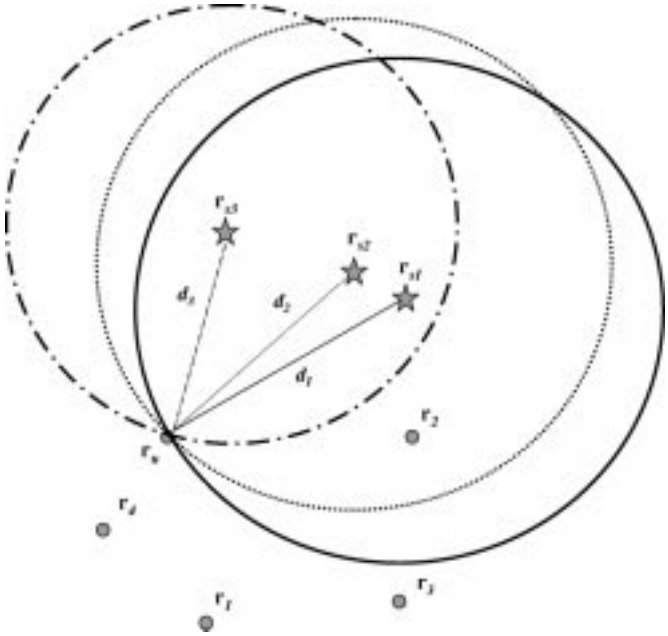

Fig. 1. Geometry of three source locations and one unknown sensor location.

may be of distinct ones or one traveling source recorded at different times. Then, the source locations $\mathbf{r}_{s_m}$ and the distances d_m are used in the LSC method to estimate the unknown sensor location.

The LSC unknown sensor location estimator is derived by expanding and manipulating the circle relations shown in Fig. 1. Consider the 2-D case, where $\mathbf{r}_{s_m} = [x_{s_m}, y_{s_m}]^T$, and $\mathbf{r}_u = [x_u, y_u]^T$. The equation of a circle from the mth source with radius d_m is given by

$$(x_u - x_{s_m})^2 + (y_u - y_{s_m})^2 = d_m^2. \quad (25)$$

By expanding the circle equation in (25) and some manipulations, we can write

$$2x_{s_m} x_u + 2y_{s_m} y_u - (x_u^2 + y_u^2) = x_{s_m}^2 + y_{s_m}^2 - d_m^2 \quad (26)$$

and in matrix form, it becomes

$$\mathbf{A}_s \begin{bmatrix} \mathbf{r}_u \\ \|\mathbf{r}_u\|^2 \end{bmatrix} = \tfrac{1}{2} \mathbf{b} \quad (27)$$

where

$$\mathbf{A}_s = \begin{bmatrix} \mathbf{r}_{s_1}^T & -\frac{1}{2} \\ \vdots & \vdots \\ \mathbf{r}_{s_M}^T & -\frac{1}{2} \end{bmatrix}, \quad \mathbf{b} = \begin{bmatrix} \|\mathbf{r}_{s_1}\|^2 - d_1^2 \\ \vdots \\ \|\mathbf{r}_{s_M}\|^2 - d_M^2 \end{bmatrix} \quad (28)$$

and $\|\mathbf{r}_u\|^2 = x_u^2 + y_u^2$. Note that (27) is also applicable for the 3-D case by defining $\mathbf{r}_{s_m}$ and $\mathbf{r}_u$ as three-dimensional (3-D) vectors. An overdetermined solution to the unknown sensor location $\mathbf{r}_u$ and $\|\mathbf{r}_u\|^2$ can be given by $(1/2)\mathbf{A}_s^{\dagger}\mathbf{b}$, where $\mathbf{A}_s^{\dagger} = (\mathbf{A}_s^T \mathbf{A}_s)^{-1} \mathbf{A}_s^T$ is the pseudoinverse of $\mathbf{A}_s$. However, when the source locations form a straight line, $\mathbf{A}_s$ degenerates, and the above formulation does not apply.

When the source locations form a straight line, e.g., a source traveling in a linear path, the circles drawn from the source locations will intersect at two locations and result in an ambiguity. However, it can be resolved if we know *a priori* that one of the intersections is a more probable candidate for the unknown sensor location. In this case, the proposed estimator needs to be slightly modified. By taking the difference of (26) for the mth source from that of the first source, we obtain

$$x_u(x_{s_m} - x_{s_1}) + y_u(y_{s_m} - y_{s_1}) = \tfrac{1}{2}\left(x_{s_m}^2 - x_{s_1}^2 + y_{s_m}^2 - y_{s_1}^2 + d_1^2 - d_m^2\right) \quad (29)$$

where $m = 2, \ldots, M$. Let $y_{s_m} = y_{s_1} = 0$ without loss of generality, e.g., source locations form a straight line on the X-axis, we obtain the estimate of the X-position of the unknown sensor by $\hat{x}_u = \mathbf{a}_x^{\dagger}\mathbf{b}_x$, where $\mathbf{a}_x = [x_{s_2} - x_{s_1}, \ldots, x_{s_M} - x_{s_1}]^T$, and $\mathbf{b}_x = (1/2)[x_{s_2}^2 - x_{s_1}^2 + d_1^2 - d_2^2, \ldots, x_{s_M}^2 - x_{s_1}^2 + d_1^2 - d_M^2]^T$. The y_u estimate is then given by the circle equations in (25) with $y_{s_m} = 0$, which becomes $(x_u - x_{s_m})^2 + y_u^2 = d_m^2$, for $m = 1, \ldots, M$. The y_u^2 estimate is given by

$$\hat{y}_u^2 = \frac{1}{M}\sum_{m=1}^{M}\left[d_m^2 - (x_u - x_{s_m})^2\right]. \quad (30)$$

If $\hat{y}_u^2$ is positive, two solutions for y_u with equal magnitude but opposite signs are given, thus providing two ambiguous unknown sensor location estimates. By having prior knowledge of which side the unknown sensor is located, the ambiguity can be resolved.

V. Simulation Examples and Evaluations

For all simulation examples and evaluations, we only consider acoustic sources. In principle, the AML method can be applied to signals of other nature, e.g., seismic, but they will not be considered for the purpose of this paper. In all cases, the sampling frequency is set to be 1 KHz. The speed of propagation is 345 m/s. A prerecorded tracked vehicle signal, with significant spectral content of about 50 Hz bandwidth centered about a dominant frequency at 100 Hz, is considered. For an arbitrary array of five sensors, we simulate the array data (with uniform gain a_p) using this tracked vehicle signal with appropriate time delays. The data length $L = 200$ (which corresponds to 0.2 s), the DFT size $N = 256$ (zero-padding), and all positive frequency bins are considered in the AML metric. In Fig. 2, the normalized $J_{\mathrm{N}}(\mathbf{r}_s)$ in (7) is evaluated at different near-field positions and plotted for a source inside the convex hull of the array (overlaid on top) under 20 dB SNR. A high peak shows up at the source location, thus indicating good estimation. When the source moves away from the array, the peak broadens and results in more range estimation error since it is more sensitive to noise. As depicted in Fig. 3 (for the same setting), the image plot of $J_{\mathrm{N}}(\mathbf{r}_s)$ evaluated at different positions show that the range estimation error is likely to occur in the source direction when the source moves away from the array. However, the angle estimation is not greatly impacted.

In the following, we consider a single traveling source scenario for a circular array (uniformly spaced on the circumference), as depicted in Fig. 4. In this case, we consider the spatial loss that is a function of the distance from the source location to each sensor location; thus, the gains a_p are no longer uniform. For each frame of $L = 200$ samples, we simulate the array data for one of the 12 source locations. We apply the AML method, assuming unity a_p, and estimate the source location at each frame. A 2-D polar grid point system is being used, where the angle is uniformly sampled, and the range is uniformly sampled in log-scale (to be physically meaningful). This 2-D grid-point search provides the initial estimate of the direct search method [28]; thus, global maximum is guaranteed. In addition, we apply the LS method [19] and the wideband MUSIC method [12] and compute the CRB using (21) for comparison purposes. Note the complexities of these methods are not compared in this paper. The wideband MUSIC divides the 200 samples into four subintervals of 50 samples each for the computation of the sample correlation matrix and uses the same grid-point search and direct search method as the AML case. As depicted in Fig. 5 [(a) for $R = 5$ and (b) for $R = 7$], both the AML and LS methods ap-

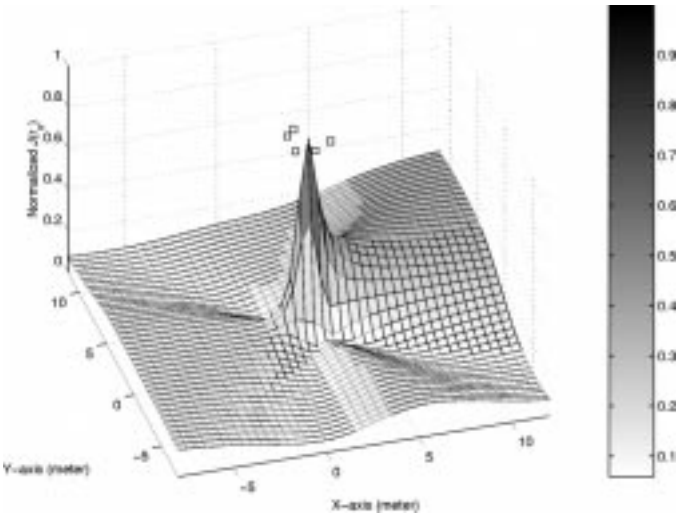

Fig. 2. Three-dimensional plot of $J_{\mathrm{N}}(\mathbf{r}_s)$ for a source inside the convex hull of the array. Square: sensor locations.

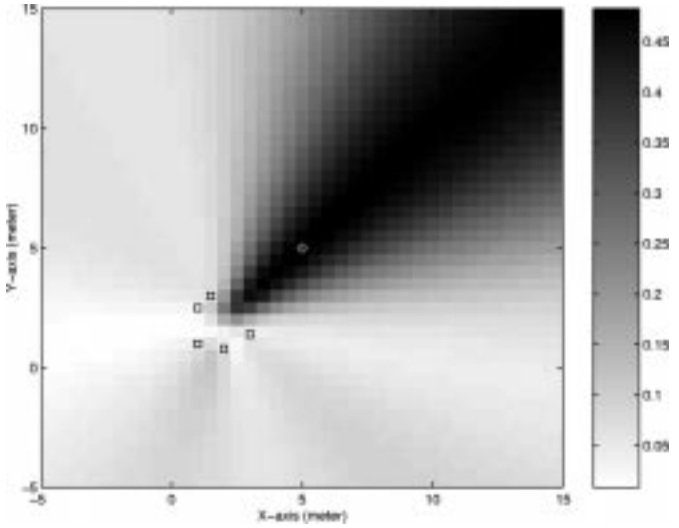

Fig. 3. Image plot of $J_{\mathrm{N}}(\mathbf{r}_s)$ for a distant source. Square: sensor locations. Circle: actual source location. $\times$: source location estimate.

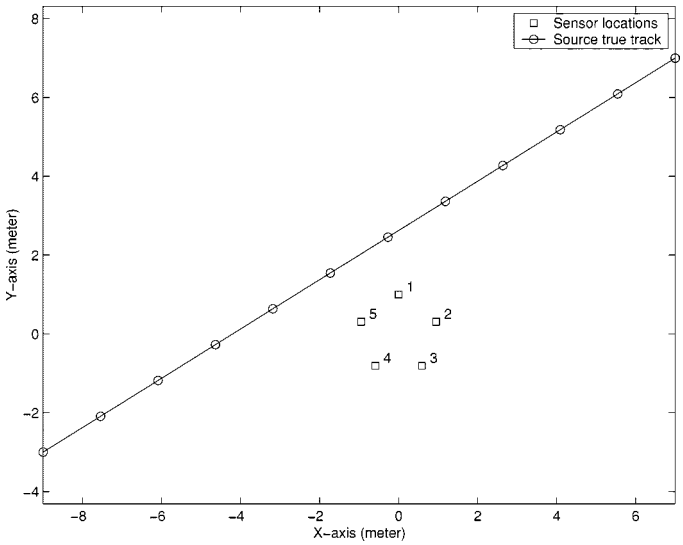

Fig. 4. Single traveling source scenario.

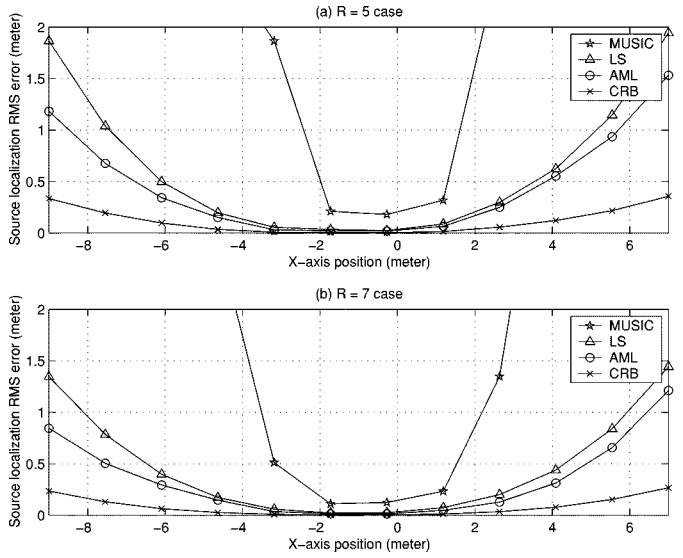

Fig. 5. Source localization performance comparison for known speed of propagation case. (a) $R = 5$. (b) $R = 7$.

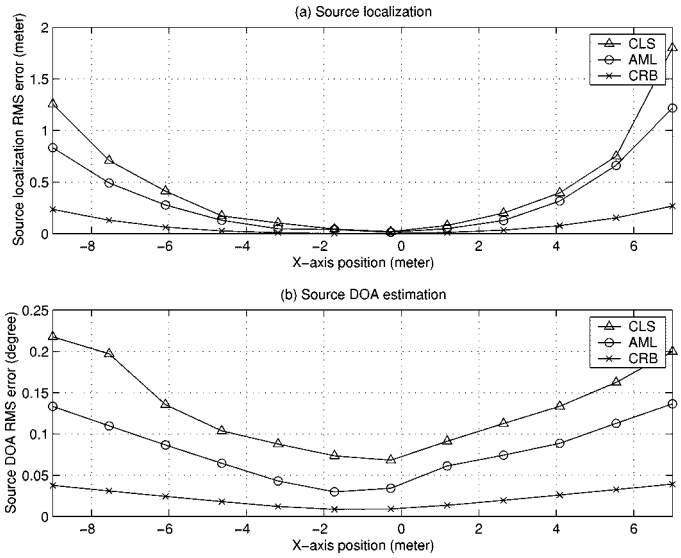

Fig. 6. (a) Source localization and (b) DOA estimations for unknown speed of propagation performance comparison ($R = 7$).

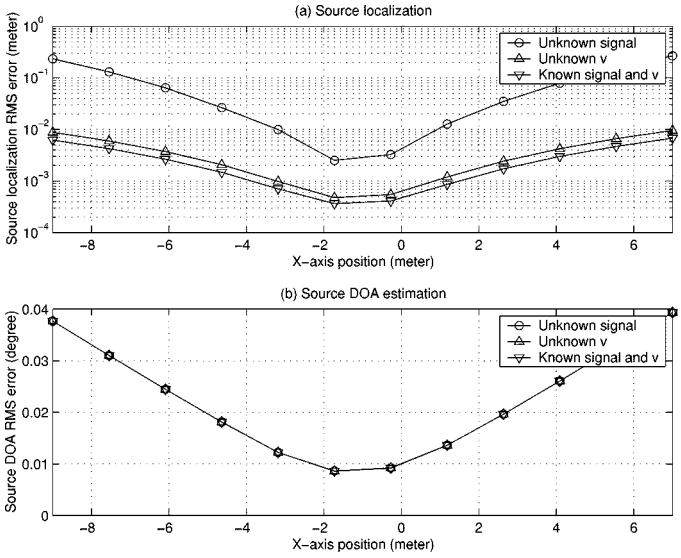

Fig. 7. CRB comparison for the traveling source scenario ($R = 7$). (a) Localization bound. (b) DOA bound.

proach the CRB when the source is near the array (high SNR and short range), but the AML outperforms the LS method. However, the wideband MUSIC yields much worse estimates than those of the LS and AML methods, especially when the source is far from the array. The wideband MUSIC requires large number of samples for good performance, but in this case, L is limited by the moving source. Note that when the source is far from the array (low SNR and long range), the CRB is too idealistic since it does not take into account other factors such as the edge effect or correlated noise across frequency. Thus, the reader should not get the impression that the AML performs poorly in this region.

When we assume that the speed of propagation is unknown, we apply the extended AML method with unknown parameters $\Theta = [\mathbf{r}_s^T, v]^T$. In this case, the CLS method in [18] is compared with the extended AML method. In Fig. 6, we show the AML method yields better overall performance in both source location and DOA estimations for $R = 7$. To compare the theoretical performance of source localization under different conditions, we compare the CRB for the known source signal and speed of propagation, unknown speed of propagation, and unknown source signal cases using seven sensors for the same single traveling source scenario. As depicted in Fig. 7, the unknown source signal is shown to have a much more significant degrading effect than the unknown speed of propagation in source location estimation. However, these parameters are not significant in the DOA estimations. Furthermore, the theoretical performance of the estimator is analyzed for different signal characteristics. For the same setting as the one shown in Fig. 3, we replace the tracked vehicle signal by a Gaussian signal after bandpass filter (with fixed SNR of 20 dB). The center frequency of the source signal is first set to 250 Hz, and then, we let the bandwidth of this signal vary from 50 to 450 Hz. As shown in Fig. 8(a), the theoretical performance improves as the bandwidth increases. Then, for a fixed bandwidth of 100 Hz, we vary the center frequency from 50 to 450 Hz and observe the performance improvement

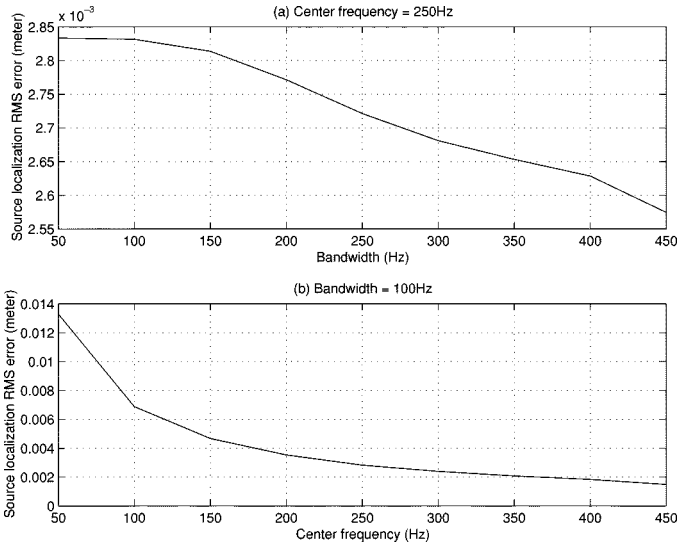

Fig. 8. CRB comparison for different signal characteristics (for scenario in Fig. 3). (a) Bandwidth. (b) Center frequency.

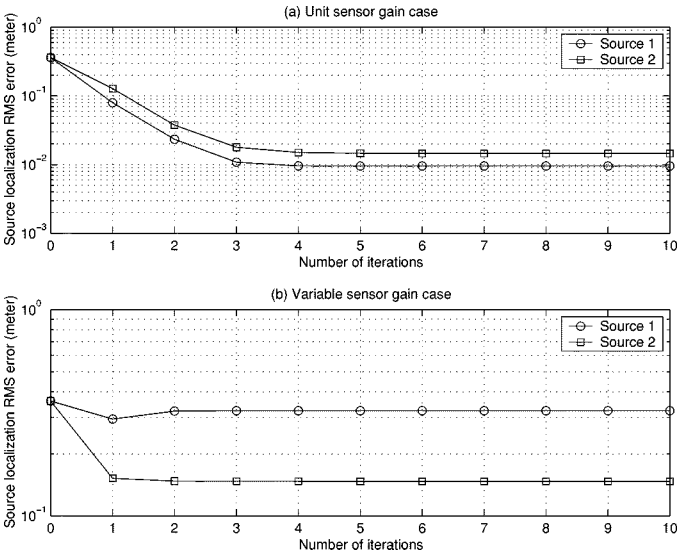

Fig. 10. RMS error of the two-source location estimates in each alternating projection iteration. (a) Unit sensor gains case. (b) Variable sensor gains case.

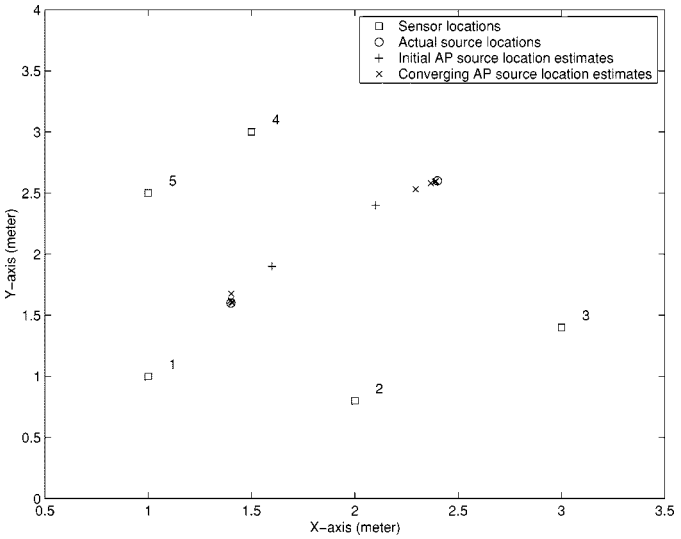

Fig. 9. Joint two-source location estimation using the AML alternating projection of five iterations (unit sensor gain case).

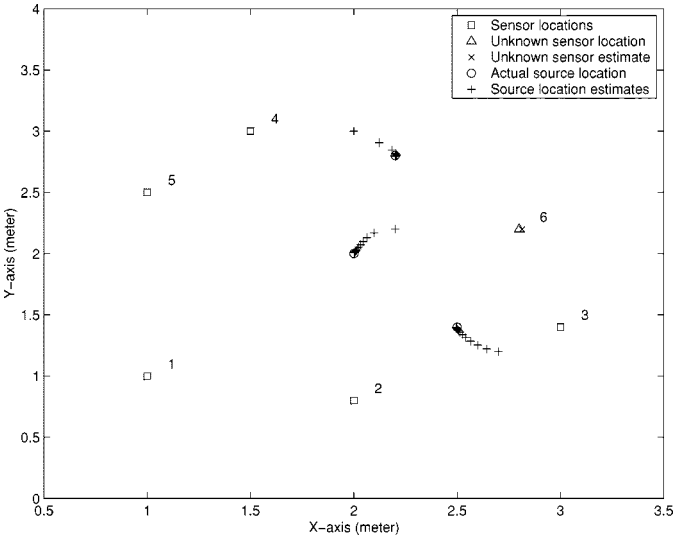

Fig. 11. Three single-source location estimations and unknown sensor location estimation.

for higher center frequency in Fig. 8(b). The theoretical performance analysis applies to the AML estimator since the AML estimator approaches the CRB asymptotically.

For two coherent sources of equal power near the array [with uniform gains $a_p^{(1)}$ and $a_p^{(2)}$], we apply the alternating projection method (10)–(13) of only five iterations for the AML method and show converging solution in Fig. 9. The same grid-point search is applied to obtain the initial estimate of one source and then the initial estimate of another source in the second step. The direct search method is applied in the following steps to reach the converging solution. In this case, the wideband MUSIC yields a false peak (not shown) since the two sources are coherent (which is a well-known problem with MUSIC-type algorithms). The RMS error of the two-source AML estimates for the first ten alternating projection iterations are plotted in Fig. 10(a) after an average of 100 realizations. The alternating projection converges in only a few iterations. However, when the sensor gains $a_p^{(m)}$ are modeled by the spatial loss and we assume they are uniform in the AML metric, the source location estimates are slightly biased, i.e., converging to an offset location, as depicted in Fig. 10(b).

To demonstrate the effectiveness of the unknown sensor location estimation method, we consider a similar scenario to the first example with one additional sensor of unknown location. As depicted in Fig. 11, the expanded parameters $[\mathbf{r}_{s_m}^T, d_m]^T$ for $M = 3$ are estimated separately using the extended AML method. From the estimated source locations and distances, the LSC method, i.e., (27), is applied, and a good estimate of the unknown sensor location is shown. Systematic evaluations via computer simulations are performed for the same scenario by placing sources uniformly within a 4×4 m^2 area around the array. The performance of the LSC using the extended AML method (which we refer to as AML-LSC) is compared with our previously proposed method using LS source location estimates

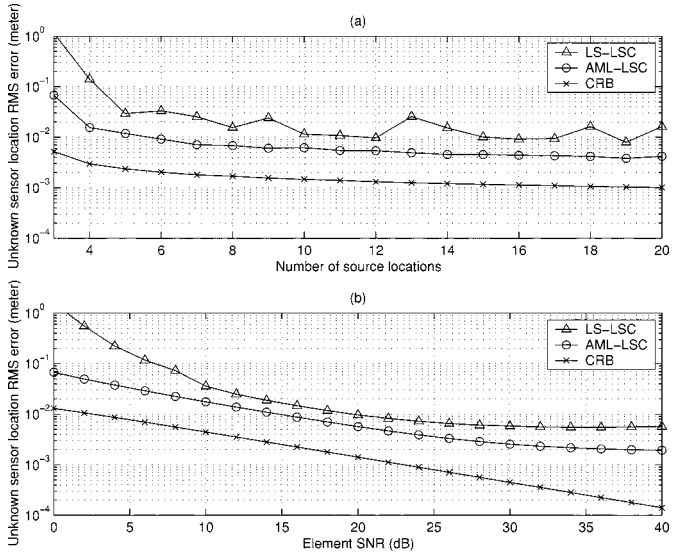

Fig. 12. Unknown sensor location estimation RMS error versus (a) number of sources and (b) SNR.

(which we refer to as LS-LSC) [26]. In Fig. 12(a), the unknown sensor location estimation RMS error is plotted with respect a different number of sources or source locations under 20 dB SNR. The proposed AML-LSC method yields improved estimates that are closer to the theoretical lower bound (derived in Appendix C). In Fig. 12(b), the RMS error is plotted with respect to the SNR for ten sources or source locations. The AML-LSC result is again better than the LS-LSC result.

VI. Conclusions

In this paper, the AML source localization solution is derived for wideband sources in the near field. In the single-source case, the AML solution maximizes the weighted cross-correlation functions of the array signal and yields the beam-steered beamformer output. We have shown its superior performance over suboptimal techniques and its efficiency with respect to the CRB. For the two-source case, we have shown good results using the alternating projection procedure of only a few iterations. We have shown that the different signal gain levels due to spatial loss are not sensitive parameters to source localization in the single-source case but are more significant in the case of multiple sources. When combining the extended AML method with the LSC unknown sensor location estimator, significant improvement is observed over other previous time-delay-based methods. The derived CRB also proves the physical observations that favor high energy in the higher frequency components of a signal. The sensitivity of source localization to different unknown parameters has also been analyzed. It has been shown that an unknown source signal results in a much larger error than that of unknown speed of propagation. The CRB supports the physical understanding of the performance in terms of the signal nature and source/array geometry.

Appendix A
Weighted Cross-Correlation Criterion

As discussed in Section II-B, the AML criterion can be shown to be equivalent to the maximum weighted cross-correlation criterion. The weighted cross-correlation function of the pth and the qth sensors is defined by

$$\begin{aligned} c_{pq}(\tau) &= \sum_{n=0}^{L-1} w_{pq} x_p(n) x_q(n-\tau) \\ &= \frac{1}{N} \sum_{k=0}^{N-1} C_{pq}(k) e^{j2\pi\tau k/N} \\ &= \frac{1}{N} \sum_{k=0}^{N-1} w_{pq} X_p(k) X_q^*(k) e^{j2\pi\tau k/N} \end{aligned} \tag{31}$$

where the weight $w_{pq} = \overline{a}_p \overline{a}_q$, $\overline{a}_p = a_p / \sqrt{\sum_{p=1}^{R} a_p^2}$ is the normalized signal gain level at the pth sensor, and $C_{pq}(k) = w_{pq} X_p(k) X_q^*(k)$ is the weighted cross-power spectral density. The maximum weighted cross-correlation criterion maximizes the sum of the weighted cross-correlation functions with the relative time delays for parameter $\mathbf{r}_s$, which can be given by

$$\begin{aligned} J_{\mathrm{wcc}}(\mathbf{r}_s) &= \sum_{p=1}^{R} \sum_{q=1}^{R} c_{pq}(t_{pq}(\mathbf{r}_s)) \\ &= \frac{1}{N} \sum_{k=0}^{N-1} \sum_{p=1}^{R} \overline{a}_p X_p(k) e^{j2\pi k t_p/N} \\ &\quad \cdot \sum_{q=1}^{R} \overline{a}_q X_q^*(k) e^{-j2\pi k t_q/N} \\ &= \frac{1}{N} \sum_{k=0}^{N-1} |B(k, \mathbf{r}_s)|^2 . \end{aligned} \tag{32}$$

Since the zero frequency bin only produces a constant term that is independent of $\mathbf{r}_s$ and the negative frequency bins are complex conjugated versions of the positive frequency bins, $J_{\mathrm{wcc}}(\mathbf{r}_s)$ is equivalent to the AML metric.

Appendix B
Extended Single-Source AML Solution for Unknown Signal Gain Level

When the a_p are unknown, we can expand the parameter space to $\Theta = [\mathbf{r}_s^T, \mathbf{S}_0^T, \mathbf{a}^T]^T$, where $\mathbf{S}_0 = [S_0(1), \ldots, S_0(N/2)]^T$ and $\mathbf{a} = [a_1, \ldots, a_R]^T$. In this case, the frequency-domain data (positive frequency bins only) is grouped into a $N/2 \times R$ data spectrum matrix $\overline{\mathbf{X}}$ with the following elements:

$$\overline{X}(k, p) = a_p S_0(k) P(k, p) + \eta_p(k) \tag{33}$$

where $P(k, p) = e^{-j2\pi k t_p/N}$ is the element of the phase matrix $\mathbf{P}$, $\eta_p(k)$ is the element of the noise matrix $\mathbf{E}$, $k = 1, \ldots, N/2$, and $p = 1, \ldots, R$. By multiplying the conjugate of the phase term on both sides of (33), we obtain the elements of the transformed data spectrum matrix as

$$\overline{X}_{\mathrm{T}}(k, p) = \overline{X}(k, p) P^*(k, p) = a_p S_0(k) + E_{\mathrm{T}}(k, p). \tag{34}$$

Note that the transformed noise matrix $\mathbf{E}_{\mathrm{T}}$ is still white Gaussian distributed with the same mean and variance. The transformed data spectrum matrix is given by $\overline{\mathbf{X}}_{\mathrm{T}} = \mathbf{S}_0\mathbf{a}^T + \mathbf{E}_{\mathrm{T}}$. By the singular value decomposition, $\overline{\mathbf{X}}_{\mathrm{T}}$ can be decomposed to

$$\overline{\mathbf{X}}_{\mathrm{T}}(\mathbf{r}_s) = \sum_{p=1}^{R} \lambda_p \mathbf{U}_p \mathbf{V}_p^H \tag{35}$$

where λ_p is the singular value, and $\mathbf{U}_p$ and $\mathbf{V}_p$ are the pth column of the left and right singular matrices, respectively. The Frobenius norm square of $\overline{\mathbf{X}}_{\mathrm{T}}$ can be given by $\|\overline{\mathbf{X}}_{\mathrm{T}}\|_{\mathrm{F}}^2 = \|\overline{\mathbf{X}}\|_{\mathrm{F}}^2 = \sum_{p=1}^{R}\lambda_p^2 = \lambda_{\max}^2 + \lambda_{\mathrm{noise}}^2$, where $\lambda_{\mathrm{noise}}^2 = \sum_{p=2}^{R}\lambda_p^2$ is the sum of the square of the noise subspace singular values. At the true source location, the square of the principle singular value corresponds to the total array signal power plus the noise power in the signal subspace. In this transformed formulation, the AML solution is given by the parameter set that minimizes the metric

$$J_{\mathrm{T}}(\Theta) = \left\|\overline{\mathbf{X}}_{\mathrm{T}}(\mathbf{r}_s) - \mathbf{S}_0\mathbf{a}^T\right\|_{\mathrm{F}}^2 \tag{36}$$

with the constraint that $\mathbf{S}_0\mathbf{a}^T$ is a rank-one matrix (i.e., outer product). At any source location $\mathbf{r}_s$, the optimal estimate of the rank-one outer product of the source spectrum vector and sensor gain vector is given by

$$\widehat{\mathbf{S}_0\mathbf{a}^T} = \lambda_{\max}\mathbf{U}_{\max}\mathbf{V}_{\max}^H \tag{37}$$

where $\mathbf{U}_{\max}$ and $\mathbf{V}_{\max}$ are the principle left and right singular vectors of $\overline{\mathbf{X}}_{\mathrm{T}}(\mathbf{r}_s)$, respectively. By substituting (37) into (36), the resulting AML metric for the source location is given by

$$\begin{aligned} J_{\mathrm{T}}(\mathbf{r}_s) &= \left\|\sum_{p=1}^{R}\lambda_p\mathbf{U}_p\mathbf{V}_p^H - \lambda_{\max}\mathbf{U}_{\max}\mathbf{V}_{\max}^H\right\|_{\mathrm{F}}^2 \\ &= \left\|\overline{\mathbf{X}}\right\|_{\mathrm{F}}^2 - \lambda_{\max}^2(\overline{\mathbf{X}}_{\mathrm{T}}(\mathbf{r}_s)). \end{aligned} \tag{38}$$

Since $\|\overline{\mathbf{X}}\|_{\mathrm{F}}$ is a constant term, we can define an equivalent metric $\tilde{J}_{\mathrm{T}}(\mathbf{r}_s) = \lambda_{\max}(\overline{\mathbf{X}}_{\mathrm{T}}(\mathbf{r}_s))$, and the source location is estimated by finding the maximum of $\tilde{J}_{\mathrm{T}}(\mathbf{r}_s)$. The normalized sensor gain vector can be estimated by $\hat{\bar{\mathbf{a}}} = |\mathbf{V}_{\max}(\overline{\mathbf{X}}_{\mathrm{T}}(\hat{\mathbf{r}}_s))|$. Note that the actual sensor gain vector $\mathbf{a}$ cannot be estimated since $\mathbf{S}_0$ is also unknown.

APPENDIX C
CRB FOR UNKNOWN SENSOR LOCATION ESTIMATION

Without loss of generality, let the sensor of unknown location be the $(R+1)$th sensor in addition to the R sensors of known locations. The array signal vector for the mth source at the kth bin can be given by $\tilde{\mathbf{X}}^{(m)}(k) = [\mathbf{X}^{(m)}(k)^T, X_u^{(m)}(k)]^T = \tilde{\mathbf{G}}^{(m)}(k) + \tilde{\eta}^{(m)}(k)$, where $\tilde{\mathbf{G}}^{(m)}(k) = [\mathbf{S}^{(m)}(k)^T, a_u^{(m)}S_0^{(m)}(k)e^{-j2\pi k t_u^{(m)}/N}]^T$, $\mathbf{S}^{(m)}(k) = \mathbf{d}^{(m)}(k)S_0^{(m)}(k)$, $a_u^{(m)}$ is the signal gain level at the sensor of unknown location, $t_u^{(m)} = \|\mathbf{r}_{s_m} - \mathbf{r}_u\|/v$ is the time-delay from the mth source to this sensor, and $\tilde{\eta}^{(m)}$ is the complex white Gaussian noise vector with variance $L\sigma^2$ in each element. By including the $N/2$ positive frequency bins and M sources, we can write the $NM(R+1)/2 \times 1$ space–temporal frequency vector as $\tilde{\mathbf{X}} = \tilde{\mathbf{G}}(\Theta) + \tilde{\xi}$, where $\tilde{\mathbf{G}} = [\tilde{\mathbf{G}}^{(1)^T}, \ldots, \tilde{\mathbf{G}}^{(M)^T}]^T$, $\tilde{\mathbf{G}}^{(m)} = [\tilde{\mathbf{G}}^{(m)}(1)^T, \ldots, \tilde{\mathbf{G}}^{(m)}(N/2)^T]^T$, and $\mathbf{R}_{\tilde{\xi}} = E[\tilde{\xi}\tilde{\xi}^H] = L\sigma^2\mathbf{I}_{NM(R+1)/2}$. The Fisher information matrix can be given by (14) with $\mathbf{H} = [\partial\tilde{\mathbf{G}}/\partial\mathbf{r}_u^T, \partial\tilde{\mathbf{G}}/\partial\tilde{\mathbf{r}}_s^T]$, where $\tilde{\mathbf{r}}_s = [\mathbf{r}_{s_1}^T, \ldots, \mathbf{r}_{s_M}^T]^T$. The resulting $D \times D$ leading submatrix of the inverse Fisher information matrix is then given by

$$\left[\mathbf{F}_{\mathbf{r}_u,\tilde{\mathbf{r}}_s}^{-1}\right]_{11:DD} = \left[\sum_{m=1}^{M}\zeta^{(m)}\left(\mathbf{A}_u^{(m)} - \mathbf{Z}_{\tilde{\mathbf{r}}_s}^{(m)}\right)\right]^{-1} \tag{39}$$

where $\zeta^{(m)} = (2/L\sigma^2v^2)\sum_{k=1}^{N/2}(2\pi k|S_0^{(m)}(k)|/N)^2$ is the scale factor for the mth source, $\mathbf{A}_u^{(m)} = a_u^{(m)^2}\mathbf{u}_u^{(m)}\mathbf{u}_u^{(m)^T}$ is the source geometry matrix, $\mathbf{u}_u^{(m)} = (\mathbf{r}_{s_m} - \mathbf{r}_u)/\|\mathbf{r}_{s_m} - \mathbf{r}_u\|$, $\mathbf{Z}_{\tilde{\mathbf{r}}_s}^{(m)} = \mathbf{A}_u^{(m)}\tilde{\mathbf{A}}^{(m)^{-1}}\mathbf{A}_u^{(m)}$ is the penalty matrix due to unknown source locations, and $\tilde{\mathbf{A}}^{(m)} = \sum_{p=1}^{R+1}a_p^{(m)^2}\mathbf{u}_p^{(m)}\mathbf{u}_p^{(m)^T}$.

The CRB for the 2-D unknown sensor location estimation variance can be given by

$$\sigma_{x_u}^2 \geq \left[\mathbf{F}_{\mathbf{r}_u,\tilde{\mathbf{r}}_s}^{-1}\right]_{11}, \quad \sigma_{y_u}^2 \geq \left[\mathbf{F}_{\mathbf{r}_u,\tilde{\mathbf{r}}_s}^{-1}\right]_{22} \tag{40}$$

and the distance error of the unknown sensor location to its true location can be given by

$$\sigma_{d_u}^2 = \sigma_{x_u}^2 + \sigma_{y_u}^2 \geq \left[\mathbf{F}_{\mathbf{r}_u,\tilde{\mathbf{r}}_s}^{-1}\right]_{11} + \left[\mathbf{F}_{\mathbf{r}_u,\tilde{\mathbf{r}}_s}^{-1}\right]_{22} \tag{41}$$

where $d_u^2 = (\hat{x}_u - x_u)^2 + (\hat{y}_u - y_u)^2$.

ACKNOWLEDGMENT

The authors would like to thank the anonymous reviewers for their valuable comments. J. C. Chen would like to thank Dr. A. G. Jaffer of Raytheon Systems for his valuable suggestions.

REFERENCES

[1] F. C. Schweppe, "Sensor array data processing for multiple signal sources," *IEEE Trans. Inform. Theory*, vol. IT-14, pp. 294–305, 1968.
[2] I. Ziskind and M. Wax, "Maximum likelihood localization of multiple sources by alternating projection," *IEEE Trans. Acoust., Speech, Signal Processing*, vol. 36, pp. 1553–1560, Oct. 1988.
[3] J. Capon, "High-resolution frequency-wavenumber spectrum analysis," *Proc. IEEE*, vol. 57, pp. 2408–2418, Aug. 1969.
[4] R. O. Schmidt, "Multiple emitter location and signal parameter estimation," *IEEE Trans. Antennas Propagat.*, vol. AP-34, pp. 276–280, Mar. 1986.
[5] S. S. Reddi, "Multiple source location—A digital approach," *IEEE Trans. Aerosp. Electron. Syst.*, vol. AES-15, Jan. 1979.
[6] J. Krim and M. Viberg, "Two decades of array signal processing research: The parametric approach," *IEEE Signal Processing Mag.*, vol. 13, pp. 67–94, July 1996.
[7] H. Wang and M. Kaveh, "Coherent signal-subspace processing for the detection and estimation of angles of arrival of multiple wideband sources," *IEEE Trans. Acoust., Speech, Signal Processing*, vol. ASSP-33, pp. 823–831, Aug. 1985.
[8] H. Hung and M. Kaveh, "Focusing matrices for coherent signal-subspace processing," *IEEE Trans. Acoust., Speech, Signal Processing*, vol. 36, pp. 1272–1281, Aug. 1988.

[9] S. Valaee and P. Kabal, "Wideband array processing using a two-sided correlation transformation," *IEEE Trans. Signal Processing*, vol. 43, pp. 160–172, Jan. 1995.
[10] J. Krolik and M. Eizenman, "Minimum variance spectral estimation for broadband source location using steered covariance matrices," in *Proc. IEEE ICASSP*, vol. 5, Apr. 1988, pp. 2841–2844.
[11] B. Friedlander and A. J. Weiss, "Direction finding for wide-band signals using an interpolated array," *IEEE Trans. Signal Processing*, vol. 41, pp. 1618–1634, Apr. 1993.
[12] T. L. Tung, K. Yao, D. Chen, R. E. Hudson, and C. W. Reed, "Source localization and spatial filtering using wideband MUSIC and maximum power beamforming for multimedia applications," in *Proc. IEEE SiPS*, Oct. 1999, pp. 625–634.
[13] H. C. Schau and A. Z. Robinson, "Passive source localization employing intersecting spherical surfaces from time-of-arrival differences," *IEEE Trans. Acoust., Speech, Signal Processing*, vol. ASSP-35, pp. 1223–1225, Aug. 1987.
[14] J. O. Smith and J. S. Abel, "Closed-form least-squares source location estimation from range-difference measurements," *IEEE Trans. Acoust., Speech, Signal Processing*, vol. ASSP-35, pp. 1661–1669, Dec. 1987.
[15] Y. T. Chan and K. C. Ho, "A simple and efficient estimator for hyperbolic location," *IEEE Trans. Signal Processing*, vol. 42, pp. 1905–1915, Aug. 1994.
[16] M. S. Brandstein, J. E. Adcock, and H. F. Silverman, "A closed-form location estimator for use with room environment microphone arrays," *IEEE Trans. Speech Audio Processing*, vol. 5, pp. 45–50, Jan. 1997.
[17] K. Yao, R. E. Hudson, C. W. Reed, D. Chen, and F. Lorenzelli, "Blind beamforming on a randomly distributed sensor array system," *IEEE J. Select. Areas Commun.*, vol. 16, pp. 1555–1567, Oct. 1998.
[18] J. C. Chen, K. Yao, R. E. Hudson, T. L. Tung, C. W. Reed, and D. Chen, "Source localization of a wideband source using a randomly distributed beamforming sensor array," in *Proc. ISIF*, Aug. 2001, pp. TuC1: 11–18.
[19] Y. Huang, J. Benesty, and G. W. Elko, "Passive acoustic source localization for video camera steering," in *Proc. IEEE ICASSP*, vol. 2, June 2000, pp. 909–912.
[20] B. Emile, P. Common, and J. Le Roux, "Estimation of time-delays with fewer sensors than sources," *IEEE Trans. Signal Processing*, vol. 46, pp. 2012–2015, July 1998.
[21] P. J. Chung, M. L. Jost, and J. F. Böhme, "Estimation of seismic wave parameters and signal detection using maximum likelihood methods," *Comput. Geosci.*, vol. 27, pp. 147–156, Mar. 2001.
[22] Y. Rockah and P. M. Schultheiss, "Array shape calibration using sources in unknown locations—I: Far-field sources," *IEEE Trans. Acoust., Speech, Signal Processing*, vol. ASSP-35, pp. 286–299, Mar. 1987.
[23] ——, "Array shape calibration using sources in unknown locations—II: Near-field sources and estimator implementation," *IEEE Trans. Acoust., Speech, Signal Processing*, vol. ASSP-35, pp. 724–735, June 1987.
[24] C. M. S. See and B. K. Poh, "Parametric sensor array calibration using measured steering vectors of uncertain locations," *IEEE Trans. Signal Processing*, vol. 47, pp. 1133–1137, Apr. 1999.
[25] S. Gazor, S. Affes, and Y. Grenier, "Wideband multi-source beamforming with adaptive array location calibration and direction finding," in *Proc. IEEE ICASSP*, vol. 3, May 1995, pp. 1904–1907.
[26] J. C. Chen, T. L. Tung, R. E. Hudson, and K. Yao, "Randomly distributed sensor self-calibration using least squares methods," in *Proc. Adv. Sensor Consort.: ARL Fed. Lab.*: , Mar. 2000, pp. 105–109.
[27] D. H. Johnson and D. E. Dudgeon, *Array Signal Processing*. Englewood Cliffs, NJ: Prentice-Hall, 1993.
[28] J. A. Nelder and R. Mead, "A simplex method for function minimization," *Comput. J.*, vol. 7, pp. 308–313, 1965.
[29] S. M. Kay, *Fundamentals of Statistical Signal Processing: Estimation Theory*. Englewood Cliffs, NJ: Prentice-Hall, 1993.
[30] T. Kailath, A. H. Sayed, and B. Hassibi, *Linear Estimation*. Englewood Cliffs, NJ: Prentice-Hall, 2000.

Joe C. Chen (S'00) was born in Taipei, Taiwan, R.O.C., in 1975. He received the B.S. (with honors), M.S., and Ph.D. degrees in electrical engineering from the University of California, Los Angeles (UCLA), in 1997 and 1998, and 2002, respectively.

Since 1997, he has been with the Sensors and Electronics Systems Group of Raytheon Systems Company (formerly Hughes Aircraft), El Segundo, CA. From 1998 to 2002, he was a Teaching Assistant at UCLA. He is currently also a part-time post-doctoral researcher at UCLA. His research interests include estimation theory and statistical signal processing as applied to sensor array systems and radar systems.

Dr. Chen is a member of the Tau Beta Pi and Eta Kappa Nu honor societies.

Ralph E. Hudson received the B.S. degree in electrical engineering from the University of California, Berkeley, in 1960 and the Ph.D. degree from the U.S. Naval Postgraduate School, Monterey, CA, in 1969.

In the U.S. Navy, he attained the rank of Lieutenant Commander and served with the Office of Naval Research and the Naval Air Systems Command. From 1973 to 1993, he was with Hughes Aircraft Company and, since then, has been a Research Associate with the Electrical Engineering Department, University of California, Los Angeles. His research interests include signal and acoustic and seismic array processing, wireless radio, and radar systems.

Dr. Hudson received the Legion of Merit and Air Medal and the Hyland Patent Award in 1992.

Kung Yao (S'59–M'65–SM'91–F'94) received the B.S.E., M.A., and Ph.D. degrees in electrical engineering from Princeton University, Princeton, NJ.

He has worked at the Princeton-Penn Accelerator, Brookhaven National Laboratory, Brookhaven, NY, and the Bell Telephone Labs, Murray Hill, NJ. He was a NASA-NRC Post-Doctoral Research Fellow at the University of California, Berkeley. He was a Visiting Assistant Professor at the Massachusetts Institute of Technology, Cambridge, and a Visiting Associate Professor at the Eindhoven Technical University, Eindhoven, The Netherlands. From 1985 to 1988, he was an Assistant Dean of the School of Engineering and Applied Science at the University of California, Los Angeles (UCLA). Presently, he is a Professor with the Electrical Engineering Department, UCLA. His research interests include sensor array systems, digital communication theory and systems, wireless radio systems, chaos communications and system theory, and digital and array signal processing. He has published more than 250 papers. He is the co-editor of *High Performance VLSI Signal Processing* (New York: IEEE Press, 1997).

Dr. Yao received the IEEE Signal Processing Society's 1993 Senior Award in VLSI Signal Processing. He was on the IEEE Information Theory Society's Board of Governors and is a member of the Signal Processing System Technical Committee of the IEEE Signal Processing Society. He has been on the editorial boards of various IEEE Transactions, with the most recent being IEEE COMMUNICATIONS LETTERS.